Journal of King Saud University - Science 36 (2024) 103353

HOSTED BY

Contents lists available at ScienceDirect

Journal of King Saud University - Science

journal homepage: www.sciencedirect.com

Full Length Article

Adroit effect of copper nanoparticles and copper nanozyme and their effective decolorization of azo dyes

R. Illakkia [a], N. Mahesh [a,*], S. Balakumar [a], N. Sivakumar [b], G.G. Kavitha Shree [c], Anand Prem Rajan [d], Chandramohan Govindasamy [e], J Aravind [f]

[a] Department of Chemistry & Biosciences, Srinivasa Ramanujan Centre, SASTRA Deemed University, Kumbakonam 612001, India
[b] Department of Molecular Microbiology, Madurai Kamaraj University, Madurai, Tamil Nadu, India
[c] Center for Post Harvest Technology, Agricultural Engineering College and Research Institute, Tamil Nadu Agricultural University, Coimbatore 641003, Tamil Nadu, India
[d] Department of Bio-Medical Sciences, School of Bio Sciences and Technology, Vellore Institute of Technology, Vellore, Tamil Nadu, India
[e] Department of Community Health Sciences, College of Applied Medical Sciences, King Saud University, P.O. Box 10219, Riyadh 11433, Saudi Arabia
[f] Department of Biotechnology, Saveetha School of Engineering, Saveetha Institute of Medical and Technical Sciences, Saveetha University, Chennai, India

ARTICLE INFO

Keywords:
Copper nanoparticle
Copper nanozyme
Degradation of mixed azo dyes

ABSTRACT

Copper nanoparticles (CuNPs) have garnered considerable attention owed to their straightforward and cost-effective synthesis techniques, making them suitable for various applications across several fields. This paper describes a straightforward method for synthesizing CuNPs using the aqueous chemical reduction approach. A unique copper nanozyme (CNZ) is also prepared to degrade dyes. The nanoparticles were analyzed using various techniques to examine their morphological structure, optical properties, functional groups, and crystallite size via SEM, UV–visible spectrophotometry, FTIR, XRD, and zeta potential with particle size analyzer. SEM analysis showed that the CuNPs have a cubical form, with particle size fluctuating from 250 to 300 nm. The CNZ has a flower-like structure with a typical 100 to 150 nm size. The zeta potential of CuNPs is measured to be + 23.4 mV, indicating a high level of stability for the nanoparticles. The XRD evaluation showed that the CuNPs displayed a prominent peak at an angle of 36.64°, indicating a crystallite size of 26.97 nm. The CNZ displayed a peak at 31.18 nm, corresponding to a crystallite size of 44.84 nm. The capacity of CuNPs and CNZ to degrade a combination of dyes (Methyl orange, Methyl red, Congo red, Tropaeolin-O, and Tartrazine) was investigated. The innovative approach utilizing CNZ and CuNPs resulted in a degradation percentage of 84.61 % for mixed colors. Experimental findings have demonstrated that the combined effect of CuNPs and CNZ is remarkably effective in catalytically degrading azo dyes, making it a highly efficient method for treating effluents from the textile sector and wastewater treatment.

1. Introduction

Persistent toxic dyes and waste products greatly impact the world's humans, flora, and fauna. These dyes are produced and consumed by various industries and release wastewater that contains hazardous dyes, which are challenging to break down because of their chemical composition, resulting in the colors being very resistant to degradation. These toxic organic dyes result in significant environmental contamination (Tsai et al. 2023; Subha et al. 2023). Several processes can degrade these harmful dyes, but they are ineffective and costly operations, these systems are prone to releasing hazardous contaminants into the water bodies. Therefore, it is decisive to practice gainful and ecologically responsive alternative approaches to reduce the issues mentioned above associated with the breakdown of colors found in wastewater (Dalal et al. 2023). Nanotechnology produces particles at the nanoscale; the atoms and molecules are manipulated. Nanoparticles are faster and lighter, can get into small spaces, and possess different properties like magnetic, electronic, and optical properties from their bulk composition in nano. Other metal and metal oxide nanoparticles are used in various fields like pharmaceuticals, cosmetics, targeted drug delivery, bioremediation, genetics, etc.; most industrial effluents discharged into the environment have become a significant cause of water pollution. They significantly affect water quality and become mutagens and carcinogens to aquatic living and human beings (Lellis et al. 2019).

* Corresponding author.
E-mail address: magi.mbbt@src.sastra.edu (N. Mahesh).

https://doi.org/10.1016/j.jksus.2024.103353
Received 16 May 2024; Received in revised form 16 June 2024; Accepted 17 July 2024
Available online 18 July 2024

These effluents contain mostly non-degraded dyes). Metal nanoparticles are the alternatives nowadays to overcome the secondary pollutants generated by traditional methods (Guerra et al. 2018; Kurhade et al. 2021; Slama et al. 2021). Copper is a transition metal with diverse physical and chemical properties (Sivayogam et al. 2021). Azo dyes are mainly employed in textile industries because of their enticing color and easy synthesis compared to natural dyes and pigments (Heydaria et al. 2017; Benkhaya et al. 2020). Azo dyes may have a single azo group (−N = N-) to n number of azo groups. These synthetic dyes released on water bodies cause foul odor and color changes in water bodies. These textile azo dyes are more soluble and difficult to remove from the water bodies (Hassan and Carr, 2018; Mariselvam et al. 2019). A CNZ is a nanostructured particle that possesses peroxidase enzyme-like activity. Hence, the name was coined as Nanozyme. It is an alternative to enzymes like horseradish peroxidase (HRP) for treating industrial effluent dyes (Batool et al. 2018; Zainal et al. 2019). The presented work uses CuNPs and CNZ to degrade an azo dye effectively. This study aims to address the research gap by developing an effective, scalable, and environmentally friendly method for azo dye degradation using the synergistic effect of CuNPs and CNZ. The combined approach leverages the catalytic properties of both materials, providing a robust solution for treating textile effluents.

2. Materials and methods

2.1. Materials

Materials used are cupric acetate, sodium hydroxide, L-ascorbic acid, copper sulfate, DL-tryptophan, phosphate buffer solution, potassium dihydrogen phosphate, sodium chloride, potassium chloride, and deionized water. The dyes Methyl red (MR), Methyl orange (MO), Congo red (CR), Tropaeolin-O (TO), and Tartrazine (TA) were acquired from Hi-media.

2.2. Preparation of copper nanoparticle (CuNPs)

CuNPs were produced by the aqueous chemical reduction technique, with a bit of adjustment to the approach described by Fathima et al. (2018). A solution containing 0.25 g of cupric acetate in 500 ml of distilled water and another solution containing 5 g of sodium hydroxide in 500 ml of distilled water while continuously stirred using a magnetic stirrer. Subsequently, a solution of L-ascorbic acid (12.5 g in 500 ml) was meticulously produced and gradually introduced into the mixture. Adding L-ascorbic acid to the copper salt solution resulted in observable changes in color, indicating the creation of CuNPs. The green solution underwent a color change to yellow and then dark brown, marking the successful production of CuNPs. The transformation into a reddish-brown color indicates the creation of CuNPs resistant to change. The solution enables the precipitation of the produced nanoparticle. Subsequently, the mixture was centrifuged and rinsed with distilled water and ethanol. After washing, nanoparticles are dried at 80 °C for 2 h. Subsequently, they are stored and utilized for further applications.

2.3. Preparation of copper nanozyme (CNZ)

The copper nanozyme (CNZ) protocol was derived from Geng et al. (2021) with minor adjustments. A 5 mM solution of PBS was created, and its pH was adjusted to 7. Next, 0.5 ml of $CuSO_4$ solution was introduced into 75 ml of PBS solution, followed by adding 1.5 ml of tryptophan solution. The solution was agitated for 15 min and left to react at ambient temperature for 24 h. The blue precipitates underwent centrifugation, were rinsed with deionized water, and were left to dry under ambient conditions for subsequent use. The DPPH test technique was used to investigate the peroxidase-like activity of CNZ.

2.4. Characterization of synthesized nanoparticle

Scanning electron microscope (SEM) on VEGA3 TESCAN characterized powder morphology, surface topography, and nanoparticle size. Stability analysis of the zeta potential was recorded on a MALVERN zeta sizer using water as a dispersant. The particle size distribution was carried out on a MALVERN particle size distributor and determined using water as a dispersant. Fourier transform infrared (FT-IR) spectra of prepared nanoparticles were documented in the range from 450 – 4000c m^{-1} KBr pellets as the reference. XRD patterns were recorded using a diffractometer with CuK_α radiation (ʎ=1.5406 Å) as a source. The crystalline size was calculated from the broadened peaks using Scherrer's formula. The average crystalline size (D) was calculated using (Eq. (1),

$$D = \frac{0.9\lambda}{B\cos\theta} \tag{1}$$

Where ʎ = X-ray wavelength (0.154 nm), Θ = Bragg diffraction angle, β= FWHM of XRD peak at angle Θ. The lattice parameter is calculated through the interplanar spacing of the planes as follows (Eq. (2):

$$a = d_{(hkl)}\sqrt{h^2 + k^2 + l^2} \tag{2}$$

Where ''a'' is the lattice parameter, d is interplanar spacing, and hkl is the Miller indices of the plane of crystal (Patil et al. 2018; Lai et al. 2022; Mohamed, 2020; Leal et al. 2024).

2.5. Catalytic degradation of mixed dyes using nanoparticles

The obtained CuNPs and CNZ were examined for dye degradation from its aqueous solution. The effect of variables like time, dye concentration, pH, temperature, and adsorbent dosage were studied. All the dyes were decolorized in an aqueous solution (Nguyen et al. 2018).

All the individual dyes' decolorization rate was initially screened with varying combinations of CNZ, CuNPs, hydrogen peroxide, and sodium borohydride. Among those combinations, CNZ, CuNPs, and hydrogen peroxide show efficient degradation of all the dyes. About 5 mg of CuNPs, 500 µl of H_2O_2, and 1 ml of CNZ (8 mg of CNZ in 1 ml of PBS) were added into 5 ml of each dye solution. The sample solution was regularly taken out, centrifuged, and analyzed using a UV–visible spectrometer to measure the absorption maximum (µmax). The percentage of degradation was calculated using the formula written below (Eq. (3).

$$Degradation\% = [(C_0 - C_t)/C_0] \times 100 \tag{3}$$

Where C_0 = initial dye concentration, C_t = final dye concentration.

3. Results & discussion

3.1. CuNPs formation

The presence of CuNPs was established by a sequence of color alterations resulting from several chemical reactions during manufacturing. Adding L-ascorbic acid to the copper salt solution results in a color change, indicating the creation of CuNPs. This color change occurs because the electrons from L-ascorbic acid cause the reduction of copper acetate to copper ions. The green solution changed from yellow to dark brown, indicating the successful creation of CuNPs. The subsequent decrease to reddish brown further confirms the development of stable CuNPs. L-ascorbic acid is a naturally occurring antioxidant that shields CuNPs from oxidation, eliminates free radicals, and is an intermediary in reduction–oxidation processes involving electron transfer (Gurav et al. 2014). Ismail et al. (2019) produced CuNPs by combining the fruit extract of *Duranta erecta*. The UV–visible spectra of the CuNP solution displayed a conspicuous absorption peak at a wavelength of

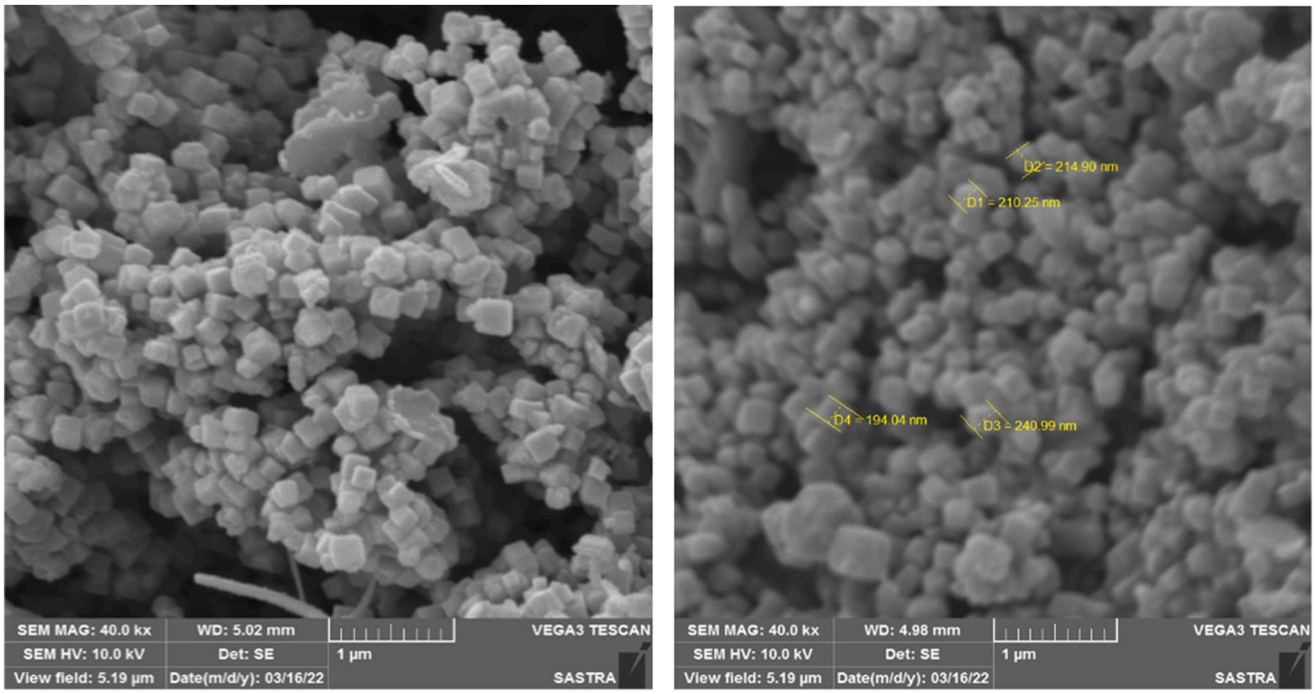

Fig. 1. SEM pictures of CuNPs.

588 nm. CuNPs were employed to reduce azo dyes and these CuNPs possess remarkable catalytic reduction properties, making them suitable for utilizing natural plant materials as affordable and environmentally acceptable substrates for CuNP synthesis. Additionally, these CuNPs can potentially be employed in the remediation of water tainted with organic dyes.

3.2. CNZ formation

The reaction of copper sulfate with PBS forms copper-phosphate residues, and the subsequent addition of tryptophan leads to the formation of a thin nanofilm, which aggregates to form a flower-like CNZ structure. After 24 h of incubation, a blue precipitate confirms the formation of CNZs. Tryptophan is crucial in arranging Cu (II)-Trp nanosheets into a flower-like structure. A similar approach was employed by Geng et al. (2021), who synthesized CNZ using a unique method. The CNZ displayed characteristic peroxidase activity towards 2, 2′-azinodi-(3-ethylbenzthiazoline)-6-sulfonate (ABTS). Comparable studies, such as those by Liu et al. (2020) and Zhang et al. (2019), also reported the synthesis of copper-based nanozymes with significant peroxidase-like

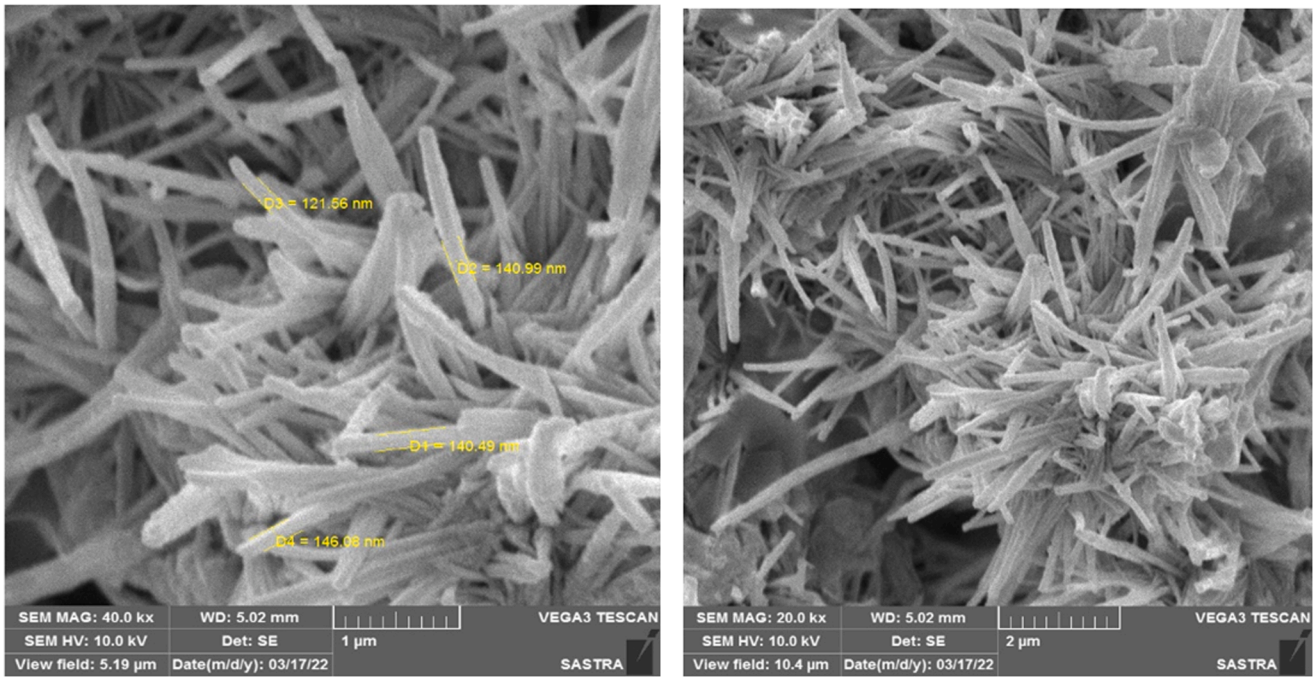

Fig. 2. SEM pictures of CNZ.

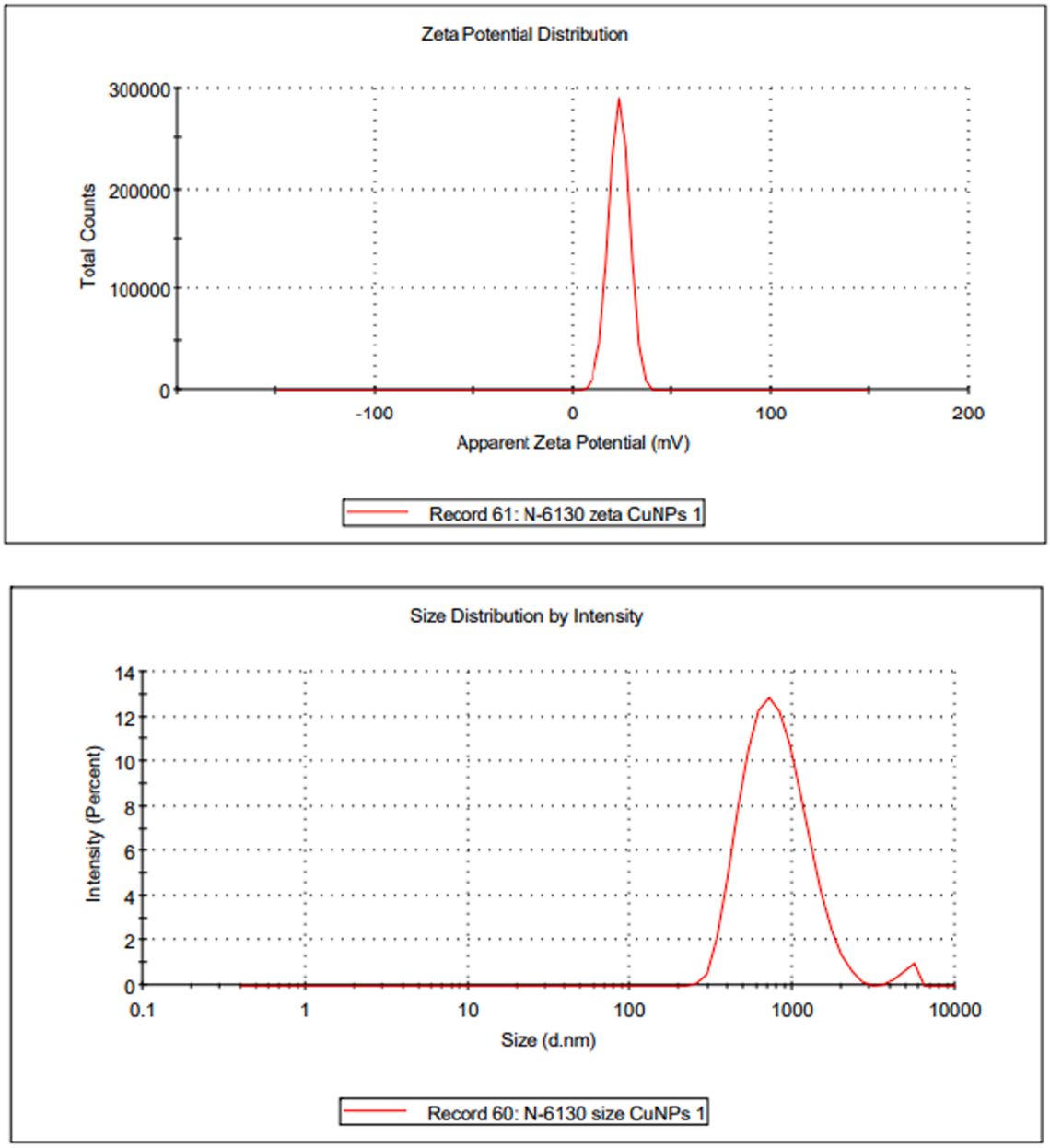

Fig. 3. Zeta potential and particle size of CuNPs.

activity. Liu et al. demonstrated the degradation of methylene blue using copper oxide nanozymes, achieving a degradation rate of 88 % under optimal conditions. Similarly, Zhang et al. reported a 90 % degradation rate of rhodamine B using CuO nanoparticles at pH 3.5 and 50 °C. In this study, CNZ was effectively utilized to degrade Methyl orange contaminants. Under conditions of pH 3.0, temperature of 60 °C, H_2O_2 concentration of 200 mM, and a CNZ dose of 8 mg, a degradation rate of 93 % was achieved in less than 10 min. This performance is superior to the 85 % degradation rate of Congo red achieved by copper nanoclusters reported by Wang et al. (2020) under similar conditions, highlighting the efficiency of the flower-like CNZ structure in catalytic applications.

Furthermore, the nanozyme demonstrated exceptional reusability and storage stability without significant degradation in performance; this aligns with the findings by Chen et al. (2021), who reported stable catalytic activity of copper-based nanozymes over multiple cycles. The high degradation rate and excellent reusability suggest that CNZ is highly effective for treating dye-containing wastewater, making it a promising candidate for industrial applications. The enhanced performance of CNZ compared to other studies may be attributed to the unique flower-like structure, which increases the surface area and active sites available for catalytic reactions. This structural advantage, combined with the synergistic effect of tryptophan in the synthesis process, results in superior catalytic efficiency.

3.3. *Peroxidase-like activity of CNZ*

The catalytic activity of CNZ was evaluated using DPPH (1,1-diphenyl-2,2-picryl-hydrazyl) as a substrate for peroxidase. It was discovered that CNZ undergoes oxidation of DPPH in the presence of H_2O_2, resulting in the formation of a solution without color. Nevertheless, DPPH cannot undergo oxidation by CNZ without H_2O_2, as shown by its purple color. The oxidation of DPPH confirms the peroxidase-like activity of CNZ into a colorless product by producing free hydroxy radicals, which results from the interaction between copper ions and

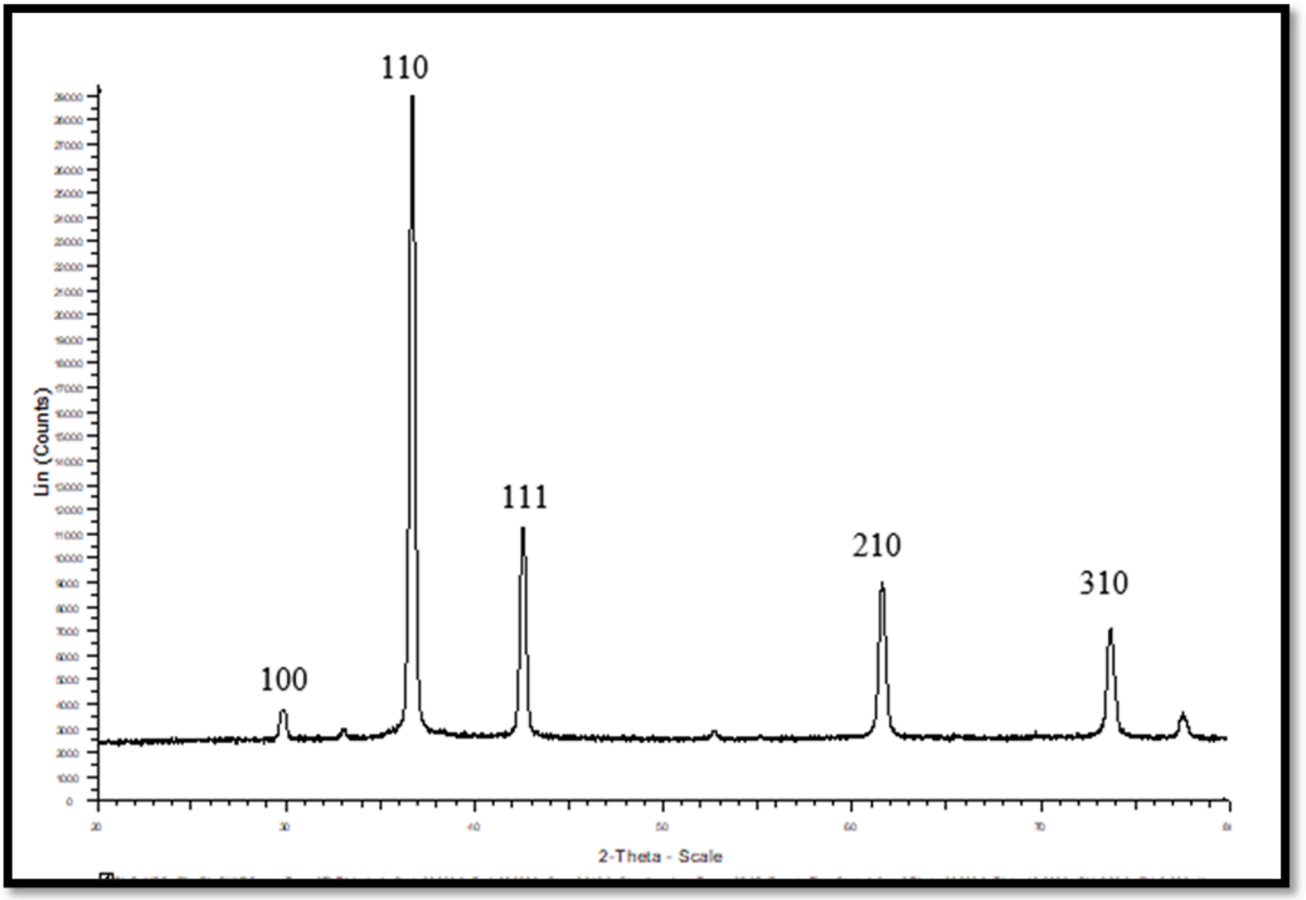

Fig. 4. XRD of CuNPs.

hydrogen peroxide. Geng et al. (2021) found that the existence of H_2O_2 leads to the oxidation of ABTS by CNZ, forming a green solution. The presence of copper ions and hydrogen peroxide (H_2O_2) can initiate a copper-redox cycle, producing the free hydroxyl radical (OH•) in a copper-redox cycle. Subsequently, this radical can undergo oxidation of ABTS, leading to the generation of a corresponding colored product. Furthermore, they evaluated the peroxidase-like functionality of copper phosphate precipitation, $CuSO_4$, and a combination of $CuSO_4$ and tryptophan. Their research showed CNZ has higher catalytic activity than copper phosphate precipitation and $CuSO_4$. The presence of tryptophan does not enhance the catalytic effectiveness of $CuSO_4$ anymore. The results suggest that the intact CNZs are accountable for the intrinsic peroxidase-like activity. The nanozyme containing copper ions had the highest enzyme-like activity, as measured.

3.4. Scanning electron microscope (SEM)

The surface morphology of the generated copper nanoparticles (CuNPs) and carbon nanotubes (CNZ) pictures are displayed in Figs. 1 and 2, respectively. The SEM was used to analyze the surface morphology of the produced CuNPs. The particles had a cubic shape and were evenly distributed, revealing copper nanoclusters with an average diameter ranging from 150 to 250 nm. The increased size results from the clustering of CuNPs in the stable phase (Conway et al. 2015) and the coating of CuNPs with a capping agent such as ascorbic acid. The scanning electron microscopy (SEM) pictures of the synthesized CNZ exhibited a floral morphology, with an average diameter ranging from 100 to 150 nm. This size falls within the nanoscale range, in contrast to the dimensions of the nanozyme previously described by Geng et al. (2021). In their work, Shubha et al. (2023) utilized FE-SEM to investigate the topological characteristics of NiO-SD NPs. The photographs of the NiO-SD nanoparticles displayed surface porosity and an irregular shape. In their study, Dawoud et al. (2020) utilized scanning electron microscopy (SEM) to examine the morphological properties of ZrO_2 and Ag-doped ZrO_2 nanoparticles. The emphasis of their investigation was on particles with a size of 1 μm. The picture showed that the microscopic particles were spherical and came together to form clusters with irregular forms that resembled monocrystals. As the concentration of dopant increases, the level of porosity also increases. Furthermore, it was noted that the particles merged and created clusters throughout the synthesis process. The roughness and cracks on the surface of the synthesized Ag-doped ZrO_2 NPs indicate that they possess porosity, which is not evident from their visual appearance.

3.5. Zeta potential and particle size

Zeta potential is employed to assess the stability of nanoparticles in a suspension. Fig. 3 depicts the zeta potential and particle size of the generated nanoparticles. Naradala et al. (2022) showed that the range of nanoparticles with excellent stability is expected to be between + 25 mV and −25 mV. The zeta potential of the synthesized CuNPs was measured to be + 23.4, suggesting a significant degree of stability. This discovery is consistent with Xiong et al.'s (2012) and Naradala et al. (2022) investigations. The average diameter of the CuNPs was measured to be 743.8 nm. The enlargement occurred due to the aggregation of nanoparticles with an average size ranging from 700 to 2000 nm in the stable phase (Conway et al., 2015). Pavani et al. (2015) observed the existence of polydisperse CuNPs, with an average diameter ranging from 600 to 680 nm. In their study, Fathima et al. (2018) utilized the dynamic light scattering (DLS) technique to determine nanoparticle dimensions and

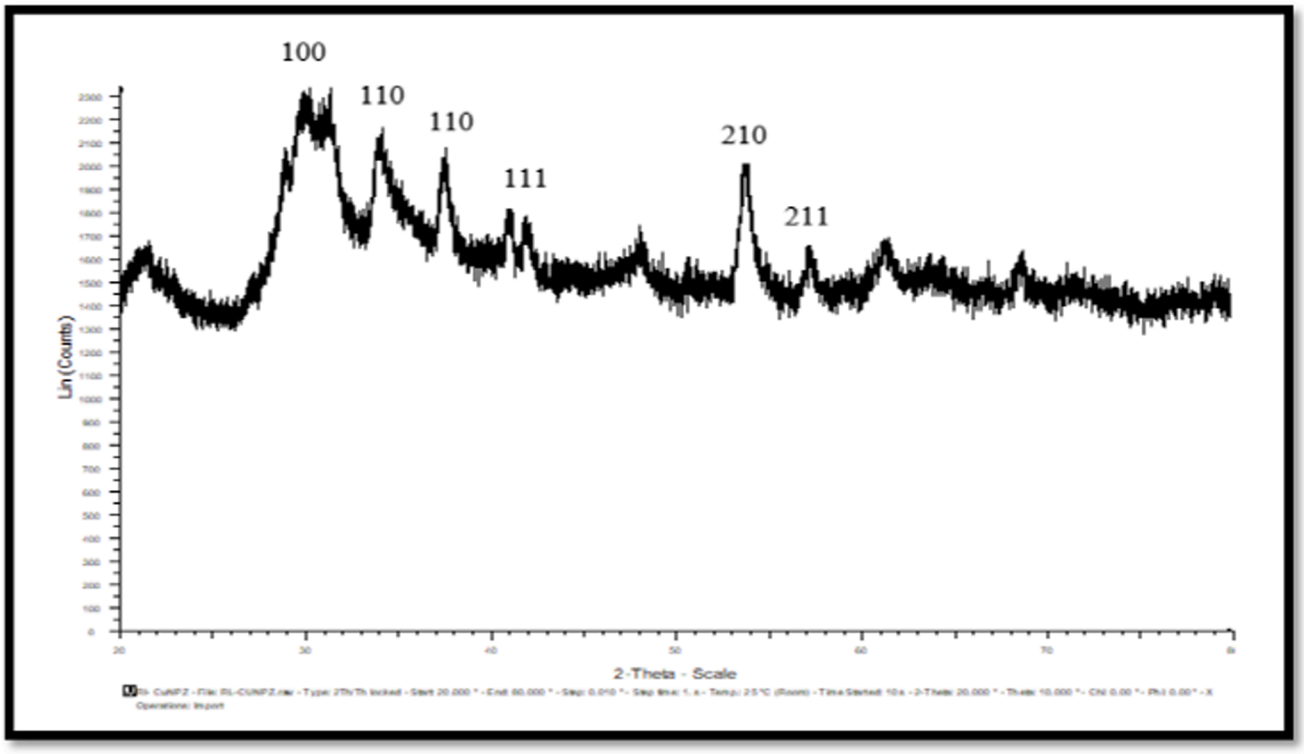

Fig. 5. XRD of CNZ.

electrical properties. The mean particle diameter and breadth were determined to be 165.2 nm and 17.73 nm, respectively. Measuring zeta potential is crucial for studying the stability of solutions that include nanoparticles. The zeta potential of the produced CuNPs was determined to be −21.9 mV.

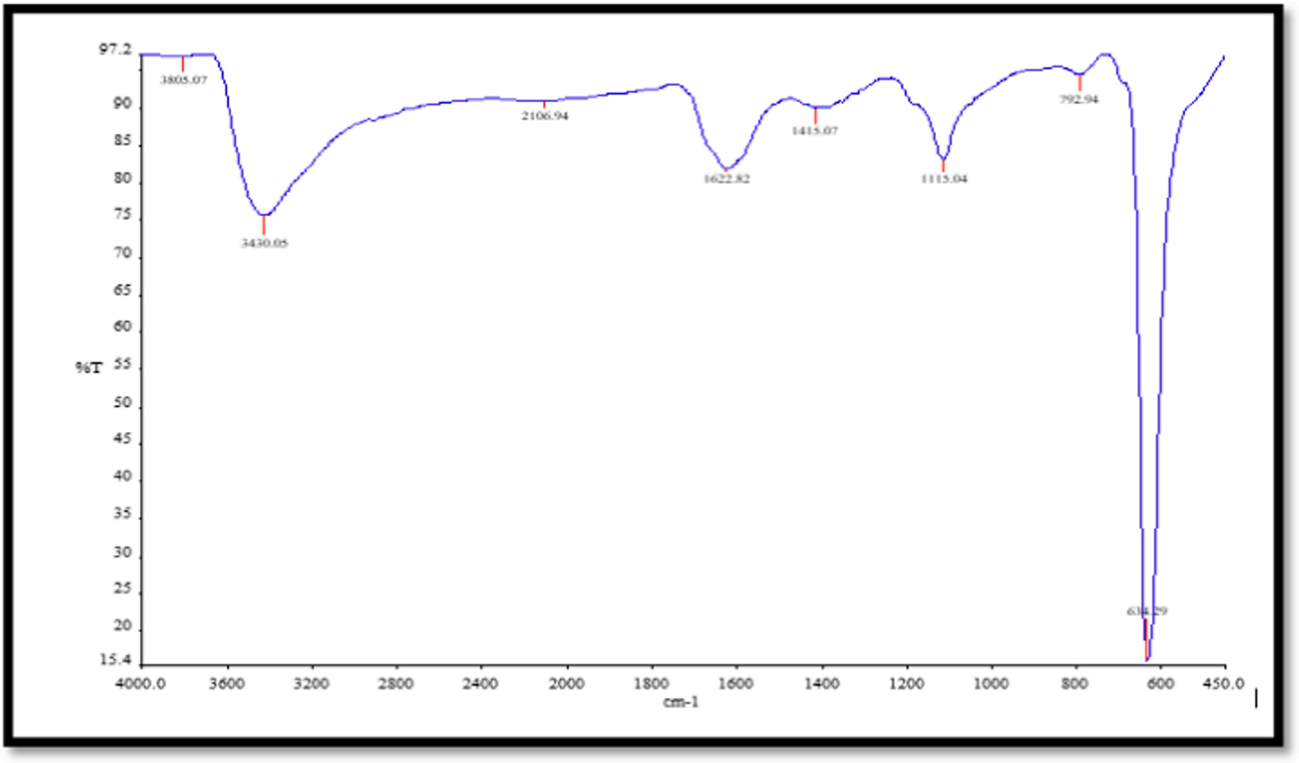

Fig. 6. FTIR CuNPs spectrum.

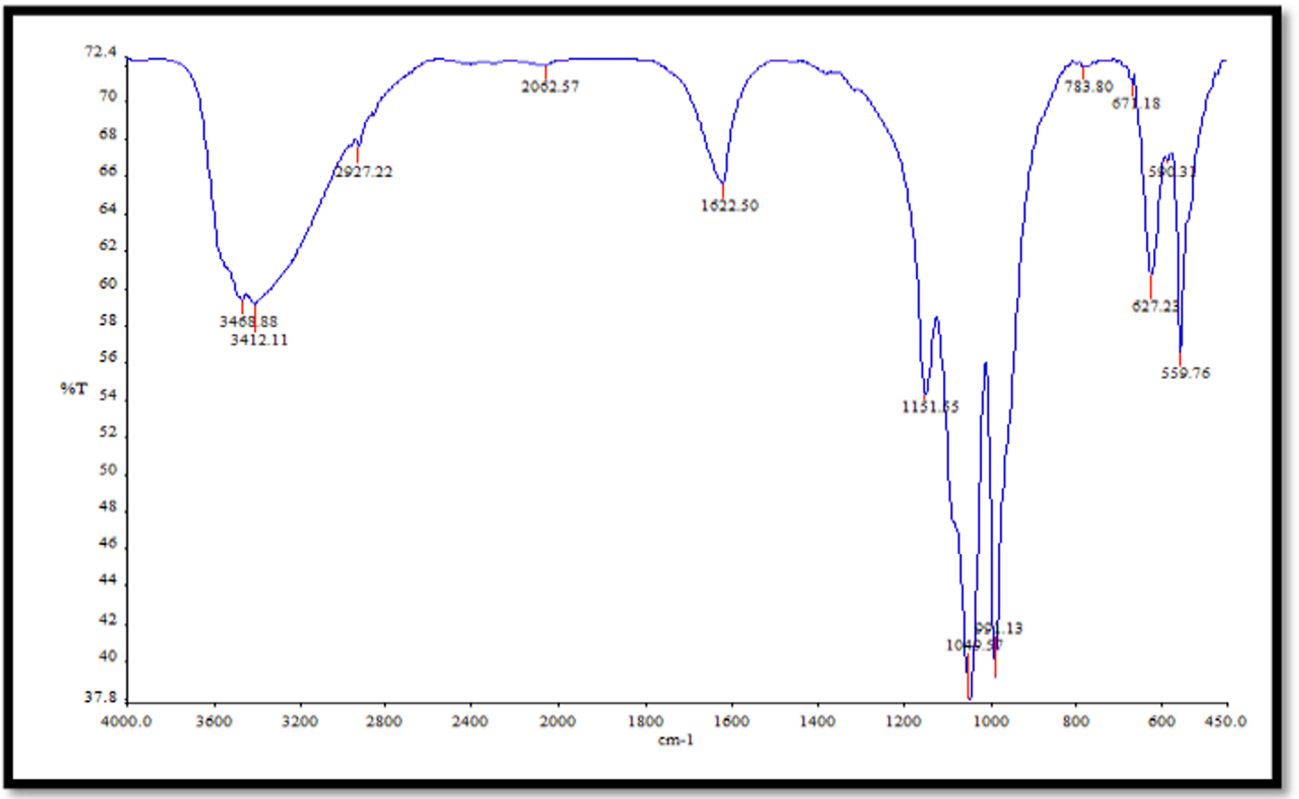

Fig. 7. FTIR CNZ spectrum.

3.6. XRD analysis

X-ray diffraction (XRD) offers precise information on the nanoparticle's crystalline structure and grain size. The XRD peaks of CuNPs were seen at 2 theta angles of 29.78, 36.64, 42.3, 52.6, 61.59, and 73.72 degrees. These peaks correspond to the crystal inter-planes of (1 0 0), (1 1 0), (1 1 1), (2 1 0), and (3 1 0). Fig. 4 displays the X-ray diffraction (XRD) pattern of CuNPs, revealing the presence of crystallite sizes within the nanometer range as shown by the widened peaks. The presence of distinct peaks in the XRD pattern indicated that the CuNPs have a crystalline structure. No peaks indicating impurities were detected, and the crystalline size was determined using Scherrer's formula based on the broadened peaks. The mean size of the crystallites was determined to be 26.97 nm. The X-ray diffraction (XRD) peaks of the CNZ (shown in Fig. 5) were seen at 2 theta angles of 28.84, 31.18, 33.99, 37.42, 41.85, 53.69, and 57.17 degrees. The corresponding inter-planar spacings were determined to be (1 0 0), (1 1 0), (1 1 0), (1 1 1), (2 1 0), and (2 1 1). The mean size of the CNZ crystals was determined to be 44.84 nm. The results exhibited a resemblance to the XRD patterns documented in previous studies. Sadia et al. (2021) provided X-ray diffraction (XRD) patterns for undoped and doped titania. Anatase titania has distinct diffraction peaks at 2θ angles of 25.2°, 37.1°, 47.5°, 53.5°, and 62.3°. The peaks exhibited similar characteristics to those found in the conventional spectrum. Regardless of the quantity of metal, the data suggested that all the samples displayed the anatase phase. The X-ray diffraction (XRD) patterns of titania samples containing metal dopants do not exhibit any identifiable diffraction peaks that correlate to the presence of the metals; this can be due to the doped metals' low concentration (1 %) and their efficient dispersion within the titania crystal phase.

3.7. FTIR spectroscopy

Figs. 6 and 7 display the FTIR spectra of CuNPs and CNZ, respectively. The FTIR spectra of the pure CuNPs exhibited a prominent peak at 3430.05 cm^{-1}, which may be ascribed to the stretching vibration of the hydrogen bond in the hydroxyl (OH) group. This peak signifies the interaction between the hydroxyl group (–OH) and the CuNPs. Additionally, a signal was seen at 1622.82 cm^{-1}, indicating the stretching vibration of the C = C bond in ascorbic acid. These potential functional groups are responsible for the synthesis and stability of CuNPs. The FTIR spectra of the compound CNZ displayed a prominent peak at a wavenumber of 3412.11 cm^{-1}. This peak was assigned to the vibrational motion of the nitrogen–hydrogen (N–H) bond inside the indole ring. A detected peak at 2972.22 cm^{-1} corresponds to the asymmetric stretching of a methyl group (CH). The presence of a peak at 1049.57 cm^{-1} suggests the occurrence of the asymmetric stretching vibration of phosphate ions, whereas a peak at 559.76 cm^{-1} indicates the bending vibration of PO_4^{3-}. The peaks exhibited a strong resemblance to the functional categories that were previously documented by Geng et al. (2021). The FTIR spectra of CuNPs and leaf extract were examined within the frequency range of 400 to 4000 cm^{-1}, as documented by Nouren et al. in 2024. The band seen at a wavenumber of 2718.11 cm-1 is attributed to the vibrational movement of the carbon-hydrogen (C–H) bond. The band seen at 1024.72 cm^{-1} corresponds to the elongation of the C–N bond in a primary amine, whereas the band at 831.71 cm^{-1} pertains to the oscillations of the C–C bond in the alkyl group found in the plant extract. The presence of lipid molecules in the leaf extract is verified by observing bands at 2354.86 cm^{-1}, which correspond to the stretching vibration of alkyne C–C bonds. The prominent absorption peak detected at 491 cm^{-1} is attributed to the vibration of metal–oxygen bonds.

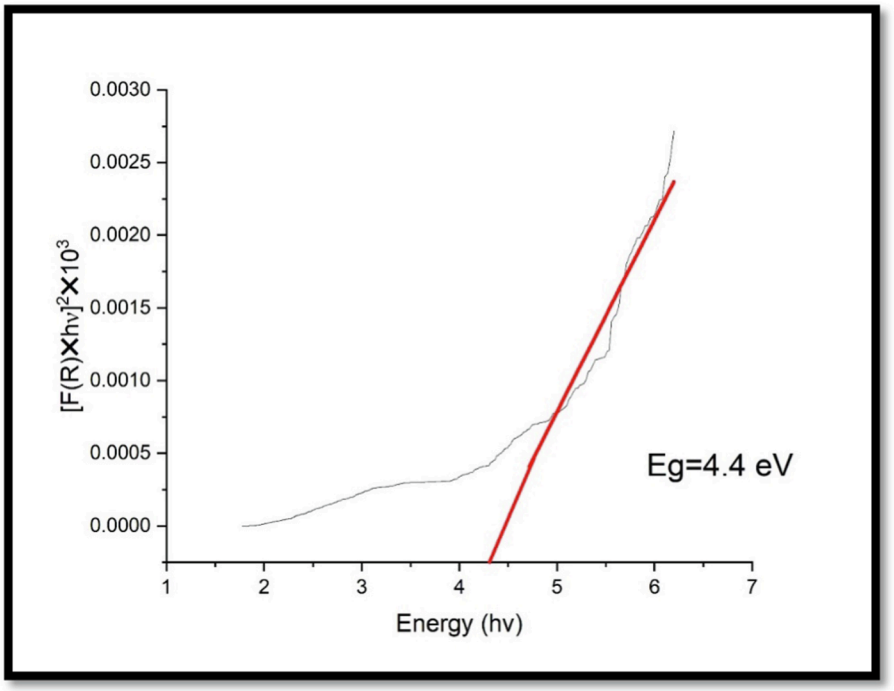

Fig. 8. Band gap for CuNPs.

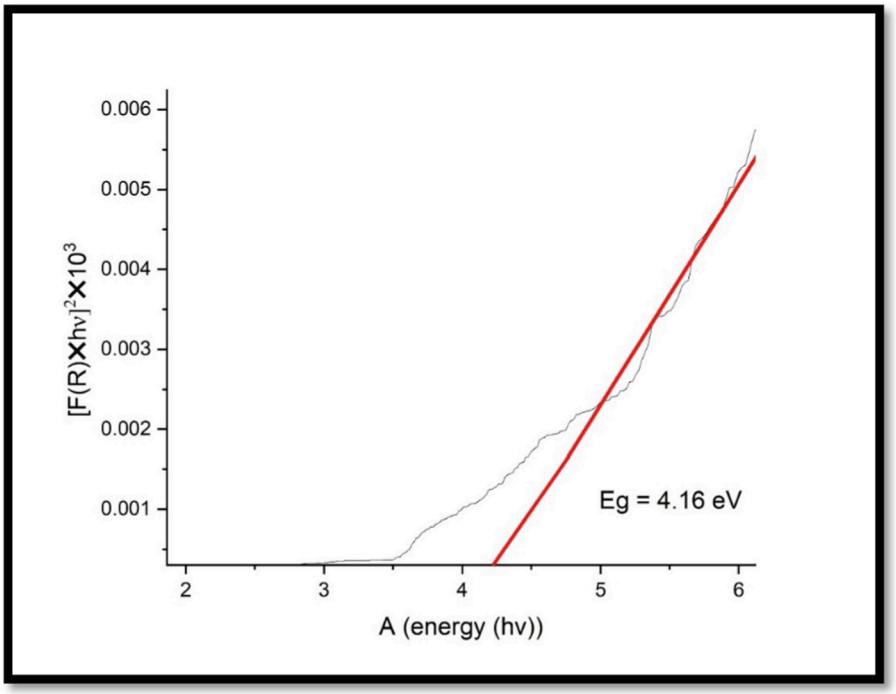

Fig. 9. Band gap for CNZ.

3.8. *Band gap energy*

Extrapolating the linear regions in the plots of $(\alpha h\upsilon)^2$ Vs photon energy ($h\upsilon$), the UV–Vis spectra of CuNPs showed high absorption in the UV wavelength region with a band gap of 4.1 eV (Fig. 8). This band gap energy is in coincides with Chandraker et al. (2020) and shows the formed CuNPs are suitable semiconductors and act as a promising photocatalyst utilized for dye degradation. The surface plasmon resonance band for CNZ (Fig. 9) was recorded, and band gap energy was calculated from the UV–Vis data. The UV–Vis spectra of CNZ showed high absorption in the UV wavelength region with a band gap of 4.4 eV.

Shubha et al. (2023) elucidated the occurrence of band-gap absorption, a phenomenon resulting from the electrical transition between Ni atoms' valence and conduction bands. The direct band gap energy of NiO-SD nanoparticles, as measured by analysis of the Tauc plot, was found to be 3.6 electron volts (eV). Dawoud et al. (2020) employed the

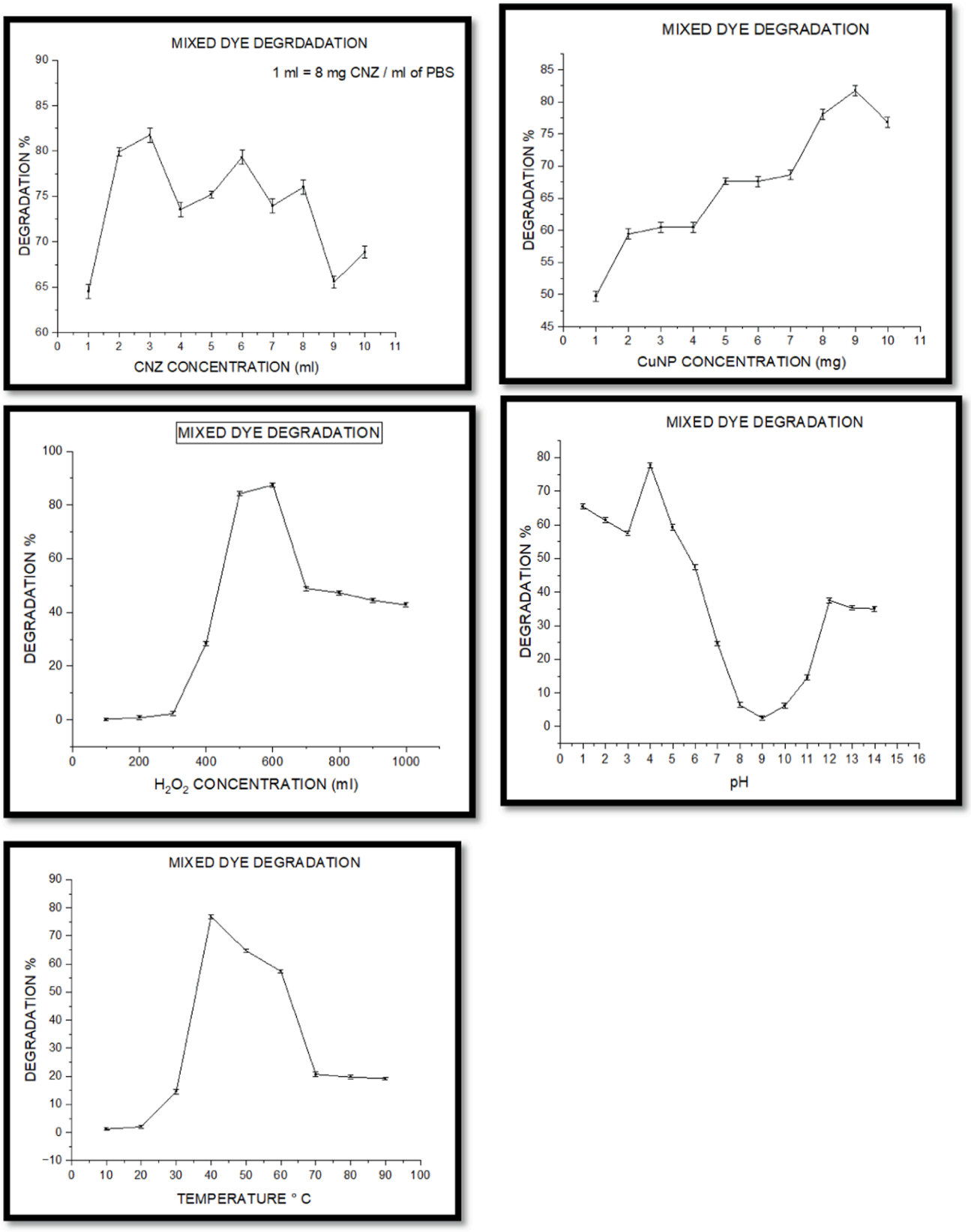

Fig. 10. Degradation of mixed dyes. (a) effect of CNZ concentration, (b) CuNPs dosage, (c) impact of H_2O_2 concentration, (d) pH, (e) temperature.

Kubelka-Munk (KM) theory to calculate the band gap (Eg). The band gap values obtained for ZrO_2 and ZrO_2 nanoparticles doped with six mol% Ag are 6 eV and 5.6 eV, respectively. The introduction of Ag-doped ZrO_2NPs led to a decrease in the band gap compared to bare ZrO_2NPs. This decrease may be explained by the transfer of energy levels from Ag to the conduction band of ZrO_2, resulting in a charge transfer.

3.9. Degradation of mixed dyes

Ffive mixed dyes (Methyl orange, Methyl red, Congo red, Tropaeolin-O, and Tartrazine) was studied, and all the parameters were evaluated for efficient degradation (Fig. 10). All the dyes are taken in 1:1:1: 1:1 ratio. The absorbance (μmax) was measured at 550 nm.

3.9.1. Optimization studies for effective dye degradation

During the initial screening of the degradation ability of azo dyes, 5 mg of CuNPs, 1 ml of CNZ, and 500 μl of hydrogen peroxide combinations reached 98–100 % of degradation within 1 h. Increased amounts of CNZ, CuNPs, or hydrogen peroxide could not improve the decolorization rate further or decrease it. Therefore, the CNZ, CuNPs, and H_2O_2 combination was chosen for the following experiments.

3.9.1.1. Effect of CNZ concentration. The consequence of CNZ dosages on mixed dyes was studied at various concentrations (Fig. 10a). The maximum degradation of about 81.76 % was achieved at 4.8 g/l of CNZ.

3.9.1.2. Effect of CuNP concentration. The effect of CuNPs was studied at various concentrations (Fig. 10b). The degradation efficiency increases with an increase in CuNPs dosage. The maximum degradation of about 81.7 % was achieved at 1.8 g/l of CuNP dosage.

3.9.1.3. Effect of hydrogen peroxide. Hydrogen peroxide can quickly produce hydroxy radicals that play a significant role in dye degradation. 120 ml of H_2O_2 /l greatly enhances the degradation process of about 87.5 % with nano-catalyst (Fig. 10c). H_2O_2 produces hydroxy radicals either by conduction band electron or by superoxide.

3.9.1.4. Effect of pH. The effect of pH on mixed dye degradation was evaluated at different pH ranging from 1 to 14. The higher efficiency of degradation of about 77.6 % is achieved at pH 4. (Fig. 10d). The degradation percent drastically decreases in neutral pH and increases from 7 to 14; this shows the process is effective in both acidic and alkaline conditions.

3.9.1.5. Effect of temperature. The optimum temperature required for maximum degradation of mixed dye was 76.84 % at 40 °C (Fig. 10e). The degradation efficiency gradually decreases when the temperature increases; this shows the degradation process is effective at an optimum temperature of 40 °C.

Dawoud et al. (2020) studied the behavior of pure ZrO2 and ZrO2 nanoparticles doped with six mol% Ag when exposed to visible light in the presence of Rh B, a cationic dye. According to the studies, the nanoparticles and other photocatalysts have exceptional photocatalytic characteristics. Indeed, a mere 150 mg of photocatalyst and a concentration of ten parts per million (ppm) of dye, when exposed for 105 min, was sufficient to destroy 95 % of Rh B. The study by Sadia et al. (2021) sought to examine the photocatalytic properties of nanoparticles. Specifically, they investigated the elimination of methylene blue and neutral red dye utilizing parent respondent material and titania doped with metal. The researchers conducted experiments to assess the impact of many attributes: pH levels, reaction duration, preliminary dye concentration, and photocatalyst, on the remediation of the dye when uncovered to UV radiation. Consequently, the deterioration of dyes increased due to the factors listed above. Using titania with Ag dopant resulted in 90 % and 95 % elimination of the two dyes. Therefore, the most effective method for discoloration industrial dye was titania doped with Ag.

Nouren et al. (2024) successfully produced copper oxide nanoparticles with photocatalytic properties utilizing a green synthesis technique, including an aqueous extract of *Jasminium sambac* leaves. Nouren et al. (2024) conducted studies to optimize copper sulfate's impacting factors. The composition of the sample, assessed using EDX analysis, revealed that it consisted of 76 % copper and 24 % oxygen. The CuO nanoparticles exhibited a crystalline structure, great crystallinity, and excellent dispersion, with a dimensions of 13 nm, and were devoid of contaminants. Furthermore, notable photocatalytic investigations have accomplished a 97 % breakdown of the dye methylene blue within 210 min.

Isa et al. (2024) employed an environmentally friendly synthesis approach to create gold nanoparticles using Johey oak fruit peel extract as a reducing and capping agent. This study examined the effect of concentrations of nanoparticles and the impact of temperatures, on the outcome. The UV-absorption spectra revealed that the Au NPs exhibited a peak absorption in the 533 to 537 nm region, which was influenced by the circumstances under which they were synthesized. The TEM analysis reveal the nanoparticles size to be 12 to 25 nm. The XRD evaluation unequivocally verified the existence of gold nanoparticles, as evidenced by the diffraction peaks aligning precisely with the established pattern. The FTIR analysis demonstrates that phytochemicals exhibit interactions with nanoparticles (NPs). The catalytic assays yielded a rate constant (RC) of 0.0795 min^{-1} for the breakdown of the rhodamine B dye in the presence of NPs and a RC of 0.0445 min^{-1} in the absence of the NPs. Therefore, this discovery suggests that the gold in nanoparticles can be employed as filters in the hybrid photovoltaic-thermal system. The study demonstrated that nanoparticles (NPs) can expedite the breakdown of contaminants, enhancing their viability in the wastewater treatment system.

4. Conclusion

The current study provided an easy fabrication, cost-effective, and convenient chemical reduction method for producing CuNPs by reducing the metal precursor in the aqueous phase and using a novel CNZ. Metallic CuNPs and CNZ were successfully synthesized and characterized with several characterization techniques such as FT-IR, XRD, Zeta potential, and SEM. Dealing azo dyes using CuNPs and CNZ is a novel method for environmental clean-up in degrading textile dyes; this was the first attempt made by the present research. The combined effect of CNZ and CuNPs efficiently degraded the mixed dyes (87.05 %). Hence, the combination of CuNPs and CNZ is a prominent catalyst for the mixed dye degradation. In the future, a pilot study on the catalytic capability of azo dyes via these CuNPs-CNZ complex will be scaled up with improved and optimized conditions for treating the dye decolorization process.

CRediT authorship contribution statement

R. Illakkia: Methodology, Investigation, Data curation. **N. Mahesh:** Software, Investigation. **S. Balakumar:** Writing – original draft. **N. Sivakumar:** Software, Investigation. **G.G. Kavitha Shree:** Validation, Software. **Anand Prem Rajan:** Visualization, Resources. **Chandramohan Govindasamy:** Funding acquisition. **J Aravind:** Writing – review & editing.

Declaration of competing interest

The authors declare that they have no known competing financial interests or personal relationships that could have appeared to influence the work reported in this paper.

Acknowledgment

This project was supported by Researchers Supporting Project number (RSPD2024R712), King Saud University, Riyadh, Saudi Arabia.

References

Batool, M., Hashmi, F., Mehboob, N., Qureshi, Z., Daoush, W.M., 2018. Studies on adsorption of Congo red (Acid Red 28) azo dye by Nano copper oxide. Advances in Nano Sciences and Nanotechnology 31 (3), 707–713.

Benkhaya, S., M'rabet, S., El Harfi, A., 2020. Classifications, properties, recent synthesis and applications of azo dyes. Heliyon 6 (1).

Chandraker, S.K., Lal, M., Ghosh, M.K., Tiwari, V., Ghorai, T.K., Shukla, R., 2020. Green synthesis of copper nanoparticles using leaf extract of *Ageratum houstonianum Mill.* and study of their photocatalytic and antibacterial activities. Nano Express 1 (1), 1–010033. https://doi.org/10.1088/2632-959X/ab8e99.

Conway, J.R., Adeleye, A.S., Gardea-Torresdey, J.G., Keller, A.A., 2015. Aggregation, Dissolution and Transformation of copper nanoparticles in Natural waters. Environ. Sci. Tech. 49 (5), 2749–2756. https://doi.org/10.1021/es504918q.

Dalal, C., Garg, A.K., Jain, N., Naziruddin, A.R., Prajapati, R.K., Choudhary, S.K., Sonkar, S.K., 2023. Sunlight-assisted photocatalytic degradation of azo-dye using zinc-sulfide embedded reduced graphene oxide. Sol. Energy 251, 315–324.

Dawoud, T.M.S., Pavitra, V., Ahmad, P., Syed, A., Nagaraju, G., 2020. Photocatalytic degradation of an organic dye using Ag doped ZrO2 nanoparticles: Milk powder facilitated eco-friendly synthesis. Journal of King Saud University – Science 32 (3), 1872–1878. https://doi.org/10.1016/j.jksus.2020.01.040.

Fathima, J.B., Pugazhendhi, A., Oves, M., Venis, R., 2018. Synthesis of eco-friendly copper nanoparticles for augmentation of catalytic degradation of organic dyes. J. Mol. Liq. 260, 1–8. https://doi.org/10.1016/j.molliq.2018.03.033.

Geng, X., Xie, X., Liang, Y., Li, Z., Yang, K., Tao, J., Zhang, H., Wang, Z., 2021. Facile fabrication of a novel copper nanozyme for efficient dye degradation. ACS Omega 6 (9), 6284–6291. https://doi.org/10.1021/acsomega.0c05925.

Guerra, E., Llompart, M., Garcia-Jares, C.G., 2018. Analysis of dyes in cosmetics: Challenges and recent developments. Cosmetics 5 (3), 47. https://doi.org/10.3390/cosmetics5030047.

Gurav, P., Naik, S.S., Ansari, K., Srinath, S., Kishore, K.A., Setty, Y.P., Sonawane, S., 2014. Colloids and Surfaces: Physiochemical and Engineering Aspects 441, 589–597.

Hassan, M.M., Carr, C.M., 2018. A critical review on recent advancements of the removal of reactive dyes from dye house effluent by ion-exchange adsorbents. Chemosphere 209 (1), 201–219.

Heydaria, R., Bastamib, F., Hosseinic, M., Alimoradib, M., 2017. Simultaneous determination of Tropaeolin O and brilliant blue in food samples after cloud point extraction. Chemical Communications Journal 5, 242–251.

Isa, E.D.M., Aid, S.R., Ali, R.R., Asako, Y., Shameli, K., Jonny, N.F.A., Yusefi, M., 2024. Green synthesis of gold nanoparticles via Artocarpus odoratissimus peel extract for potential applications of optical filter and catalytic degradation. *Journal of King Saud University* –. Science 103209.

Ismail, M., Gul, S., Khan, M.I., Khan, M.A., Asiri, A.M., Khan, S.B., 2019. Green synthesis of zerovalent copper nanoparticles for efficient reduction of toxic azo dyes Congo red and methyl orange. Green Process. Synth, 8 (1), 135–143. https://doi.org/10.1515/gps-2018-0038.

Kurhade, P., Kodape, S., Choudhury, R., 2021. Overview on green synthesis of metallic nanoparticles. Chem. Pap. 75 (10), 5187–5222.

Lai, M.J., Huang, Y.W., Chen, H.C., Tsao, L.I., Chang Chien, C.F., Singh, B., Liu, B.R., 2022. Effect of size and concentration of copper nanoparticles on the antimicrobial activity in Escherichia coli through multiple mechanisms. Nanomaterials 12 (21), 3715.

Leal, M.V.G., Gomes, A.S., Tolosa, G.R., Bachmann, C., Dognani, G., Osorio-Román, I., Job, A.E., 2024. Synthesis of cellulose-copper nanoparticle (cCMF/CuNPs) hybrid material for photodegradation of Congo red dye. Cellul. 31 (2), 1039–1051.

Lellis, B., Fávaro-Polonio, C.Z.F., Pamphile, J.A., Polonio, J.C., 2019. Effects of textile dyes on health and the environment and bioremediation potential of living organisms. Biotechnology Research and Innovation 3 (2), 275–290. https://doi.org/10.1016/j.biori.2019.09.001.

Mariselvam, R., Ranjitsingh, A.J.A., Thamaraiselvi, C., S. j., 2019. Degradation of azo dye using plants based silver nanoparticles through ultraviolet radiation. *Journal of King Saud University* –. Science 31 (4), 1363–1365. https://doi.org/10.1016/j.jksus.2019.07.001.

Mohamed, E.A., 2020. Green synthesis of copper & copper oxide nanoparticles using the extract of seedless dates. Heliyon 6 (1).

Naradala, J., Allam, A., Tumu, V.R., Rjaboina, R.K., 2022. Antibacterial activity of copper nanoparticles synthesized by *Bambusa arundinacea* leaves extract. Biointerface Research in Applied Chemistry 12 (1), 1230–1236.

Nguyen, C.H., Fu, C.-C., Juang, R.-S., 2018. Degradation of methylene blue and methyl orange by palladium-doped TiO2 photocatalysis for water reuse: Efficiency and degradation pathways. J. Clean. Prod. 202, 413–427. https://doi.org/10.1016/j.jclepro.2018.08.110.

Nouren, S., Bibi, I., Kausar, A., Sultan, M., Nawaz Bhatti, H.N., Safa, Y., Sadaf, S., Alwadai, N., Iqbal, M., 2024. Green synthesis of CuO nanoparticles using Jasmin sambac extract: Conditions optimization and photocatalytic degradation of methylene blue dye. *Journal of King Saud University* –. Science 36 (3), 103089. https://doi.org/10.1016/j.jksus.2024.103089.

Patil, S.B., Ravishankar, T.N., Lingaraju, K., Raghu, G.K., Nagaraju, G., 2018. Multiple applications of combustion derived nickel oxide nanoparticles. J. Mater. Sci. Mater. Electron. 29 (1), 277–287. https://doi.org/10.1007/s10854-017-7914-2.

Sadia, M., Naz, R., Khan, J., Zahoor, M., Ullah, R., Khan, R., Naz, S., Almoallim, H.S., Alharbi, S.A., 2021. Metal doped titania nanoparticles as efficient photocatalyst for dyes degradation. *Journal of King Saud University* –. Science 33 (2), 101312. https://doi.org/10.1016/j.jksus.2020.101312.

Shubha, J.P., Savitha, H.S., Patil, R.C., Assal, M.E., Shaik, M.R., Kuniyil, M., Alduhaish, O., Dubasi, N., Farooq Adil, S.F., 2023. A green approach for the degradation of toxic textile dyes by nickel oxide (NiO-SD) NPs: Photocatalytic and kinetic approach. *Journal of King Saud University* –. Science 35 (7), 102784. https://doi.org/10.1016/j.jksus.2023.102784.

Slama, H.B., Chenari Bouket, A., Pourhassan, Z., Alenezi, F.N., Silini, A., Cherif-Silini, H., Belbahri, L., 2021. Diversity of synthetic dyes from textile industries, discharge impacts and treatment methods. Appl. Sci. 11 (14), 6255.

Tsai, M.J., Chung, M.Y., Kuo, M.Y., Wu, J.Y., 2023. Effective enhancement of performances on photo-assisted dye degradation using a Zn coordination polymer and its post-modified Cu/Zn bimetallic analogue under natural environments. J. Environ. Chem. Eng. 11 (2), 109258.